JOURNAL OF GEOPHYSICAL RESEARCH, VOL. 111, A08206, doi:10.1029/2005JA011450, 2006

Computing magnetospheric mass density from field line resonances in a realistic magnetic field geometry

D. Berube,[1] M. B. Moldwin,[1,2] and M. Ahn[1]

Received 30 September 2005; revised 6 March 2006; accepted 20 April 2006; published 24 August 2006.

[1] Ultra-low-frequency (ULF) field line resonances can be used to infer the mass density along magnetospheric magnetic field lines. By specifying how mass density is distributed along the magnetic field (usually a power law as a function of distance from the Earth) and a dipole magnetic field geometry, the MHD standing wave equation can be analytically solved and mass density inferred from observed field line eigenfrequencies. However, the geometry of the Earth's magnetic field can deviate significantly from a dipole, even at relatively low L shells and on the dayside magnetosphere. This study investigates the importance of including a realistic magnetic field geometry when computing plasma mass density from observed field line eigenfrequencies. A generalized version of the toroidal mode MHD standing wave equation is solved using the Tsyganenko (2002a, 2002b) empirical magnetic field model (T01). The results are compared to those found using a dipole. We find that assuming a dipole magnetic field geometry results in an overestimation of mass density. The overestimation is larger for more disturbed levels of geomagnetic activity. Our results have important implications for the inference of heavy ions in the magnetosphere. Namely, an increase in heavy ion concentration as a result of enhanced geomagnetic activity will be exaggerated unless the proper magnetic field geometry is taken into account when calculating mass density from field line eigenfrequencies.

Citation: Berube, D., M. B. Moldwin, and M. Ahn (2006), Computing magnetospheric mass density from field line resonances in a realistic magnetic field geometry, *J. Geophys. Res.*, *111*, A08206, doi:10.1029/2005JA011450.

1. Introduction

[2] Observations of ultra-low-frequency (ULF) field line resonances (FLRs) have been used for decades to infer the mass density along magnetospheric field lines [e.g., *Troitskaya and Gul'elmi*, 1967; *Takahashi and McPherron*, 1982; *Menk et al.*, 1999; *Denton et al.*, 2001]. The earliest researchers were able to use numerical integration to solve the MHD standing wave equation by assuming a dipole magnetic field geometry and a power law (as a function of radial distance from the Earth) distribution of mass density along field lines [e.g., *Cummings et al.*, 1969; *Orr and Matthew*, 1971]. A technique for numerically solving the wave equation in an arbitrary magnetic field was first introduced by *Singer et al.* [1981]. Since then, the Singer et al. technique has been used for a variety of magnetic field models and density distributions [*Waters et al.*, 1996; *Hattingh and Sutcliffe*, 1987; *Denton et al.*, 2001; *Rankin and Tikhonchuk*, 2001; *Wanliss et al.*, 2002].

[3] The resonant frequencies (eigenfrequencies) of a closed magnetic field line (i.e., one with both ends fixed in the ionosphere) depend on its length, the strength of the magnetic field, and the surrounding plasma mass density. In the plasmasphere and plasmatrough regions, techniques have been developed to measure these frequencies using ground-based magnetometers [*Baransky et al.*, 1985, 1989; *Waters et al.*, 1991, 1995]. Meridional chains of closely spaced magnetometers can be used to determine field line resonance frequency as a function of latitude [*Pilipenko and Federov*, 1994; *Kawano et al.*, 2002]. The main advantage of ground magnetometer techniques is that they allow continuous monitoring of FLRs, and thus plasma mass density, whenever a resonance is present. However, care must be used when inverting the measured frequencies to obtain mass density because the process involves assumptions of the magnetic field geometry and the distribution of mass along the field line. The purpose of this study is to investigate the importance of a realistic magnetic field geometry versus the usual dipole field assumption when using FLRs to determine plasma mass density.

[4] The inner magnetospheric magnetic field is often approximated as a dipole. This is primarily because until recently, no empirical model existed which attempted to accurately describe the magnetic field there as a function of solar wind conditions. The T01 model [*Tsyganenko*, 2002a, 2002b] was developed to specifically model the near-Earth magnetosphere. The main improvement of T01 over earlier magnetic field models with respect to modeling the inner magnetosphere is that it includes a more accurate representation of the ring current. The T01 ring current takes into account the axisymmetric component as well as a partial ring current with field-aligned closure currents [*Tsyganenko*, 2002a]. Using the T01 model, *Tsyganenko et al.* [2003]

[1]Department of Earth and Space Sciences, University of California, Los Angeles, California, USA.
[2]Also at Institute of Geophysics and Planetary Physics, University of California, Los Angeles, California, USA.

0148-0227/06/2005JA011450$09.00

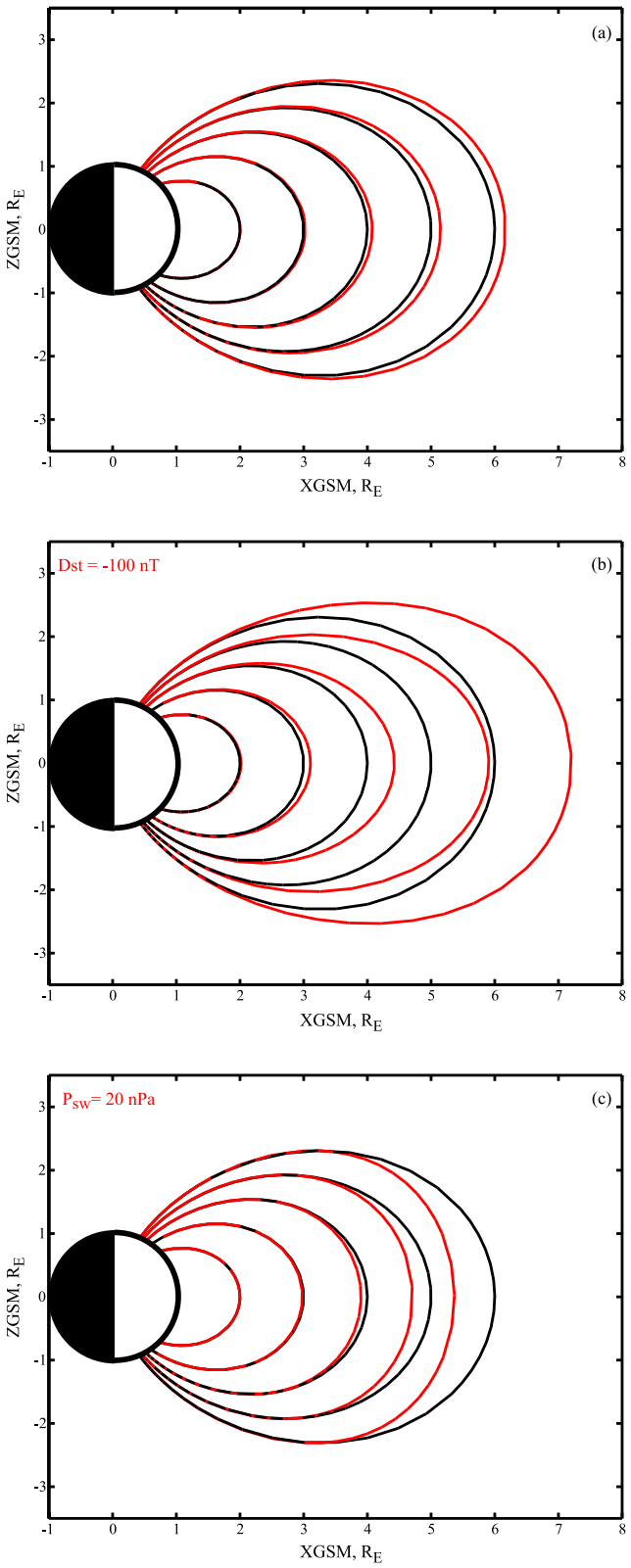

Figure 1. Dipole field lines (black) and T01 model field lines (red) plotted at noon MLT for (a) average solar wind conditions, (b) *Dst* = −100 nT, and (c) P_{sw} = 20 nPa.

showed that the dipole approximation can break down as close as 3–4 R_E on the nightside during the main phase of large geomagnetic storms.

[5] The remainder of this paper is organized in the following way: In section 2 we compare the geometry of T01 field lines to a dipole as a function of local time, *L* shell, and geomagnetic activity. In section 3 we use the *Singer et al.* [1981] technique to solve the MHD standing wave equation and determine the eigenfrequencies of inner magnetospheric field lines. The conditions under which T01-determined eigenfrequencies differ significantly from those determined assuming a dipole are discussed. In section 4 the database of dayside FLRs constructed by *Berube et al.* [2005] is utilized to statistically compare plasma mass density computed from the T01 model using the *Singer et al.* [1981] technique to density computed assuming a dipole field. Conclusions are presented in section 5.

2. Geometry of T01 Versus Dipole Field Lines

[6] The T01 model is an empirical model of the inner and near magnetosphere (X_{GSM} >= −15 R_E). The inputs to the model are the solar wind dynamic pressure P_{sw}, the *Dst* index, IMF B_y and B_z, Earth's dipole tilt angle, and two parameters G_1 and G_2. G_1 and G_2 are functions of the solar wind speed V_{sw} and magnetic field strength and are used to parameterize the cross-tail current (see *Tsyganenko* [2002b] for a complete description of these terms). The Earth's internal field $\mathbf{B}_{int}$ can be calculated using the International Geophysical Reference Field (IGRF) or a dipole. For a given location inside the magnetosphere, the total field strength is calculated as $\mathbf{B}_{tot} = \mathbf{B}_{int} + \mathbf{B}_{T01}$.

[7] The geometry of T01 field lines can differ significantly from that of a dipole depending on the inputs to the model. The "partial" effects of variations of different input parameters on the geometry of magnetospheric magnetic field lines were shown by *Tsyganenko* [2002b] (see Figure 11 of that paper). Here we perform a similar calculation for field lines typically passing through the plasmasphere.

[8] Figure 1a shows dipole field lines at noon MLT for *L* = 2–6 plotted in black. The red lines are field lines plotted from the same northern hemisphere footpoints using T01 with average solar wind conditions as inputs (P_{sw} = 2 nPa, *Dst* = −20 nT, IMF B_z = IMF B_y = 0 nT). For average conditions, there is not a significant difference in the geometry of T01 field lines versus that of a dipole. The equatorial crossing points of the T01 field lines only differ by a fraction of a R_E from the dipole field lines. The difference in field line length between a dipole and T01 is also quite small.

[9] Figure 1b shows the same dipole field lines as Figure 1a plotted in black, and T01 field lines using the same input parameters as 1a except with *Dst* = −100 nT. For this case, there is a significant effect on both field line length and equatorial crossing point beyond *L* = 4. The T01 field lines are stretched due to the effect of the ring current included in the model. In Figure 1b, the dipole field line that crosses the equator at 6 R_E instead crosses it at 7.2 R_E.

[10] Figure 1c shows the same dipole field lines as Figure 1a plotted in black, and T01 field lines using the same input parameters as 1a except with P_{sw} increased to 20 nPa. The increase in dynamic pressure compresses the

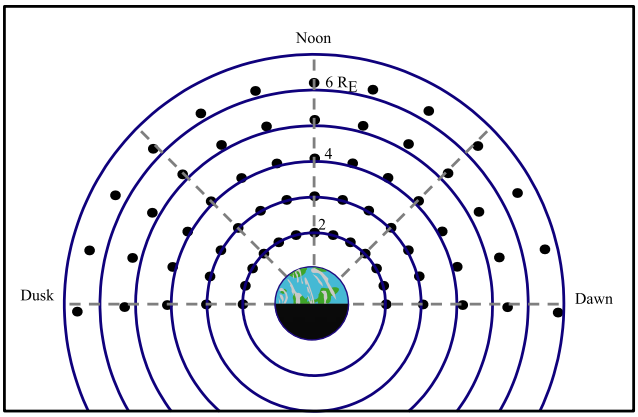

Figure 2. Equatorial crossing radii of T01 model field lines with the same footpoints as dipole field lines for L = 2–6. The inputs to the model are the same as Figure 1a.

magnetosphere and field lines cross the equator closer to the Earth than their dipole counterparts. For instance, the L = 6 field line crosses the equator at 5.5 R_E.

[11] The solar wind dynamic pressure greatly influences the strength of the magnetopause current system, whereas *Dst* determines the strength of the ring current. Since the ring current is located in the inner magnetosphere, the geometry of inner magnetospheric field lines is influenced more by *Dst* than by P_{sw}. Comparing Figures 1b and 1c, we see that this is indeed the case. Therefore we expect that changes in field line resonance frequency due to changes in field line geometry will correlate best with *Dst.*

[12] Since T01 takes into account the interaction of the solar wind with the magnetosphere as well as the local time asymmetry of the ring current, we expect differences in the geometry of dipole versus T01 field lines as a function of local time. These differences are illustrated in Figure 2, which shows the equatorial plane viewed from above the North Pole. The concentric circles are at 2, 3, 4, 5, and 6 R_E. The black points represent the equatorial crossing points of the L = 2, 3, 4, 5, and 6 field lines for each hour from 0600 to 1800 MLT, calculated using T01 with the same input parameters as Figure 1a. A local time effect is apparent beyond 3 R_E. The T01 field line equatorial crossing points are farther from the Earth than their dipole counterparts, with the largest differences toward both dawn and dusk. Also, the figure shows that near dawn (dusk), the local time where the field line crosses the equator is earlier (later) than the local time where the field line leaves the surface of the Earth, due to the fact that field lines are swept antisunward by the solar wind.

[13] A quantitative analysis of the effects of varying solar wind conditions and local time differences on field line resonance frequencies and corresponding mass densities is presented in section 3.

3. FLR Frequencies of T01 Versus Dipole Field Lines

[14] The toroidal mode equation for standing waves in an arbitrary magnetic field is given by *Singer et al.* [1981],

$$\frac{\partial^2}{\partial s^2}\xi' + \frac{\partial}{\partial s}\left(\ln\left(h_\alpha^2 B\right)\right)\frac{\partial}{\partial s}\xi' + \frac{\omega^2}{V_A^2}\xi' = 0. \qquad (1)$$

In equation (1), s is the coordinate representing the distance along the field line (i.e., s = 0 is the foot of the field line), B is the magnetic field, V_A is the Alfvén speed, ω is the angular eigenfrequency, the scale factor h_α is the distance to an adjacent field line in the azimuthal direction, and ξ' is the linear displacement in the azimuthal direction divided by h_α.

[15] We want to compare eigenfrequencies and mass densities determined from solving the *Singer et al.* equation using the T01 model to those determined assuming a dipole. We assume a power law distribution of mass density along field lines of the form

$$\rho = \rho_{eq}\left(\frac{R_{\max}}{R}\right)^m, \qquad (2)$$

where ρ is the mass density, ρ_{eq} is the density at the equator, R is the distance from the center of the Earth to the location along the field line, R_{max} is the maximum distance, and m is the power law dependence. Empirical studies of the field line dependence of mass density in the plasmasphere have found m (sometimes denoted by α) ranges from 0 to 6 [e.g., *Takahashi and McPherron*, 1982; *Menk et al.*, 1999; *Gallagher et al.*, 2000]. Other recent studies have found the density to be fairly constant along plasmaspheric field lines over a wide range of latitudes around the equator, suggesting a value of m close to zero [*Goldstein et al.*, 2001; *Reinisch et al.*, 2001; *Takahashi et al.*, 2004]. In fact, the radial distance (R in the equation above) does not vary significantly over a large portion of the field line surrounding the equator. Thus the value of m chosen when computing density from observed field line resonance frequencies results in an uncertainty in density smaller than that associated with the measured frequency. For instance, at L = 2.5, the difference in the computed equatorial density between choosing m = 0 and m = 3 from a frequency of 20 mHz is 16 percent, whereas the typical uncertainty in density that arises from determining the frequency from the data is around 25 percent [e.g., *Berube et al.*, 2003]. We note that there are situations when the assumption of a power law distribution may not be appropriate, such as at very low latitudes (L < 2) where a significant portion of the field line is in the ionosphere. Techniques which do not assume a functional dependence of density along field lines have been developed [*Price et al.*, 1999], but those techniques require observations of several harmonic frequencies, which are rarely seen in ground data. This study's main focus is the role magnetic topology plays in the determination of mass density from observed field line resonance frequencies. Our choice of a power law distribution of mass density along field lines allows the results of this study to be compared to other previous results where a power law was assumed. The quantitative effects of choosing different functional forms for the mass density dependence will be the topic of a future study.

[16] The Alfvén speed in equation (1) depends on both the magnetic field and mass density. Using the expression for mass density from equation (2),

$$V_A^2 = \frac{B^2}{\mu_0\rho} = \frac{B^2}{\mu_0\rho_{eq}}\left(\frac{R_{\max}}{R}\right)^{-m}, \qquad (3)$$

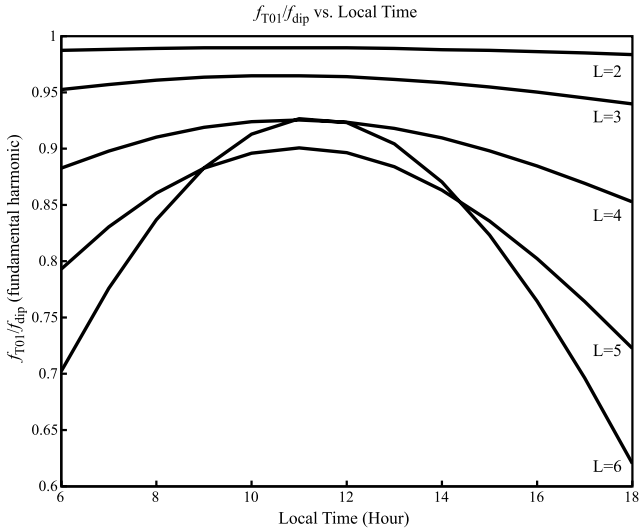

Figure 3. Ratio of the fundamental field line eigenfrequency determined using T01 to that found assuming a dipole versus local time. The inputs to the model are the same as Figure 1a.

equation (1) becomes

$$\frac{\partial^2}{\partial s^2}\xi' + \frac{\partial}{\partial s}\left(\ln\left(h_\alpha^2 B\right)\right)\frac{\partial}{\partial s}\xi' + \frac{\mu_0\omega^2\rho_{eq}}{B^2}\left(\frac{R_{\max}}{R}\right)^m \xi' = 0. \quad (4)$$

The magnetic field B, radial distance R, and h_α can all be expressed in terms of the field line coordinate *s*. Identifying

$$P(s) = \frac{\partial}{\partial s}\left(\ln\left(h_\alpha^2 B\right)\right) \quad (5)$$

and

$$Q(s) = \frac{\mu_0\rho_{eq}}{B^2}\left(\frac{R_{\max}}{R}\right)^m, \quad (6)$$

equation (4) can be written as

$$\frac{\partial^2}{\partial s^2}\xi' + P(s)\frac{\partial}{\partial s}\xi' + \omega^2 Q(s)\xi' = 0. \quad (7)$$

The set of eigenvalues of equation (7) are the field line eigenfrequencies squared. We can solve for ω^2 by providing appropriate boundary conditions and numerically integrating along the field line. Since the field line is assumed to be fixed at its ionospheric endpoints, the wave amplitude must be zero there. Therefore we choose $\xi' = 0$ there.

[17] For a given equatorial mass density, we solve for the eigenfrequency using a simple shooting code. The field line coordinate *s*, magnetic field strength B, and h_α are determined using the T01 model. We start at one end of the field line with an initial guess for ω and solve for ξ' at the other end by numerically integrating equation (7) along the field line using a fourth-order Runge-Kutta method. The value of ω is adjusted and the integration repeated until ξ' at the other end is within a specified tolerance. The code will solve for the harmonic nearest to the initial guess. The process can be repeated several times with different initial guesses to solve for multiple harmonics.

[18] Assuming a mass density of 1 amu cm^{-3} everywhere in the magnetosphere (i.e., a power law dependence with $m = 0$), we calculated the fundamental harmonic frequency for the $L = 2-6$ field lines for each hour from 0600 to 1800 magnetic local time using the T01 magnetic field model and the average solar wind input parameters that were used in Figure 1a. Figure 3 is a plot of the ratio of the fundamental harmonic computed using T01 to the fundamental harmonic computed assuming a dipole magnetic field (we use the notation f_{T01}/f_{dip}). The largest differences are found near dawn and dusk, especially for field lines beyond $L = 4$. Also note that the curves are not symmetric about 1200 LT due to the fact that the ring current in the T01 model includes a dawn-dusk asymmetry. The differences are not as significant below $L = 4$. Another important feature of Figure 3 is that for all field lines, f_{T01} is smaller than f_{dip}. This means that assuming a dipole results in a systematic overestimation of mass density, since frequency and density are inversely proportional to one another.

[19] Under the dipole assumption, any change in the field line resonance frequency can only be attributed to a change in mass density along the field line, since the field line geometry does not change. In reality, a changing resonance frequency can be due to changing field line geometry, changing mass density, or both. Figure 4 is a plot of contours of constant f_{T01}/f_{dip} at noon MLT for *L* shells from 2 to 6 and *Dst* from −200 nT to 50 nT. Again we have assumed a constant mass density of 1 amu cm^{-3} everywhere in the magnetosphere. The plot shows that at *L* shells as low as $L = 4$, the eigenfrequency for a given density can be significantly less than the expected eigenfrequency assuming a dipole solely due to an increase in geomagnetic activity. This has important implications for inferring plasma mass density changes during geomagnetic storms. As an example, suppose we observe the eigenfrequency for a particular field line decrease during the main phase of a storm. Under the dipole

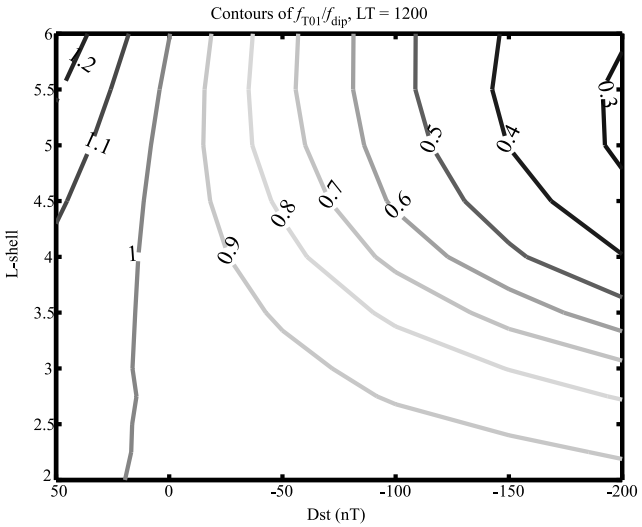

Figure 4. Contours of f_{T01}/f_{dip} for *L* shells from 2 to 6. The inputs to the model are the same as Figure 1a, except *Dst* varies from 50 to −200 nT.

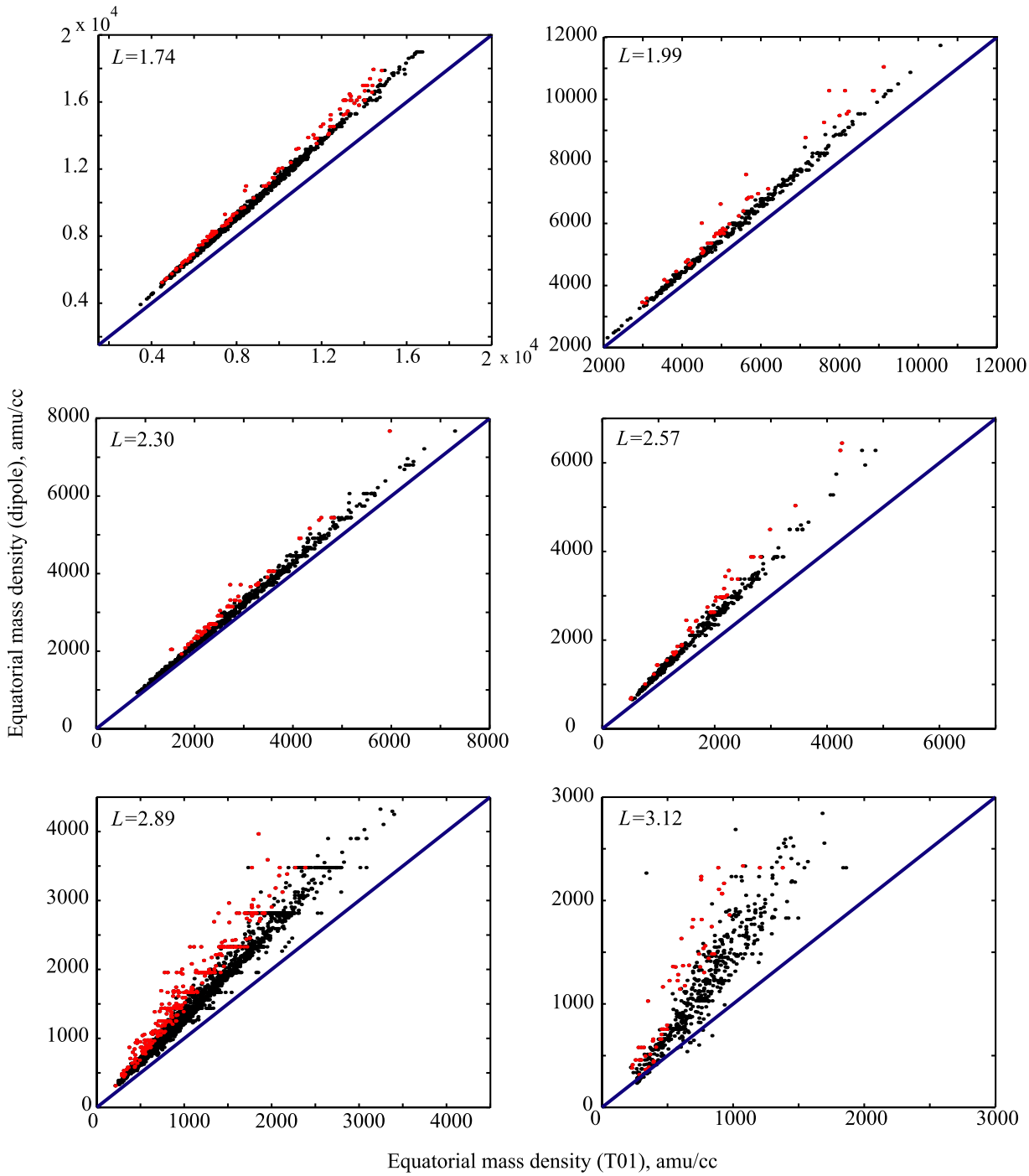

Figure 5. Equatorial mass density computed assuming a dipole magnetic field versus the density computed using the T01 model for six pairs of stations in the MEASURE array of ground magnetometers. The blue line represents perfect agreement between a dipole and the model. The red points are times when $Dst < -50$ nT.

assumption, the observed decrease in frequency can only be explained by an increase in mass density along the field line. Figure 4 shows that the decrease could partly be explained by the fact that the field line geometry is also changing. The important implication of this result is that in order to use field line resonances to monitor plasma mass density dynamics, field line geometry must be taken into account, even for field lines inside the plasmasphere, where the dipole assumption is commonly used during geomagnetic storms.

4. Mass Density Determined From Observed Eigenfrequencies Using T01

[20] In the previous section, we assumed a density distribution and solved equation (7) for field line eigenfre-

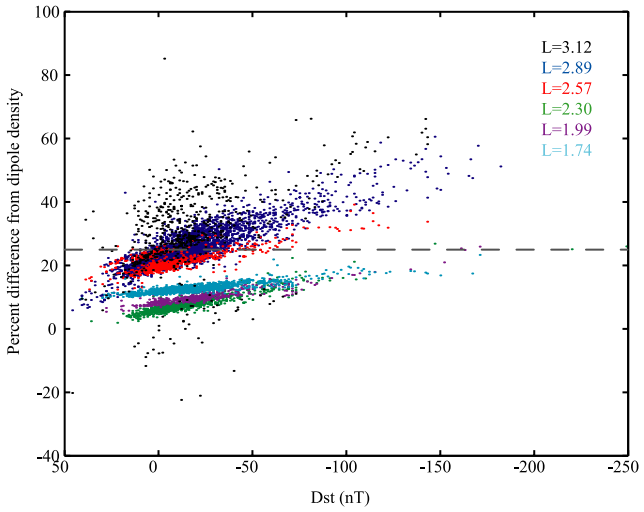

Figure 6. Percent difference between mass density computed assuming a dipole and density computed using the T01 plotted versus *Dst* for the six pairs of MEASURE stations used in this study.

quencies. In practice, the frequencies are observed and we want to determine the density. In that case, ρ_{eq} and ω^2 can be swapped in equation (6) and equation (7), and equation (7) can be solved for ρ_{eq} using the same scheme described in section 3.

[21] *Berube et al.* [2005] developed an empirical plasmaspheric mass density model from approximately 5200 hours of field line resonance frequencies measured using pairs of stations from the MEASURE chain of magnetometers (http://measure.igpp.ucla.edu). The array contains pairs of stations with midpoints at L = 1.74, 1.99, 2.30, 2.57, 2.89, and 3.12. Equatorial mass density was calculated assuming a dipole magnetic field and a power law distribution of mass density with m = 3.

[22] In order to compare mass density determined assuming a dipole to that determined using T01, we solved equation (7) using the same database of FLRs as *Berube et al.* [2005], for the same distribution of mass density as in that study. Solar wind inputs to the T01 model were obtained using NASA Space Physics Data Facility's OMNIWEB (http://omniweb.gsfc.nasa.gov) service. Figure 5 shows plots comparing the density computed by *Berube et al.* [2005] to density computed using T01 for the six station pairs. The solid line represents perfect agreement between the two data sets. The red points represent times with $Dst < -50$ nT.

[23] Figure 5 clearly shows that the dipole assumption results in an overestimation of mass density at all station pairs, with the exception of a few points for the L = 3.12 pair. The agreement between dipole and T01 densities is worse for large values of *Dst* (<−50 nT) as shown by the red points. The MEASURE data only extend to L = 3.12, but the large amount of scatter present in the comparison for that pair (bottom right panel of Figure 5) suggests that the difference between dipole and T01-determined densities is much less predictable at larger L, which is reasonable considering the fact external conditions will have a larger effect on the geometry of field lines which extend farther out into the magnetosphere. Below L = 3, the difference between using a dipole and T01 is almost negligible, except for large densities and disturbed conditions.

[24] The uncertainty in determining field line eigenfrequencies using pairs of ground stations results in an uncertainty in mass density of 25 percent or less [*Berube et al.*, 2003]. The difference in density between a dipole and T01 is often much greater than 25 percent. Figure 6 plots this difference as a function of the level of geomagnetic activity. The figure shows the percent difference in density between a dipole and T01 for the six station pairs plotted versus *Dst*. Even for moderately disturbed ($Dst = -50$ nT) geomagnetic activity and field lines below L = 3, the difference can be larger than the maximum uncertainty associated with determining the field line eigenfrequency. Such large differences imply that the dipole assumption can lead to a significant over estimation of mass density for these conditions, and the change in field line geometry associated with changing geomagnetic conditions must be taken into account when determining mass density from FLRs in the plasmasphere.

5. Summary and Conclusions

[25] We have investigated the importance of choosing a realistic magnetic field geometry in relation to the problem of determining the mass density along magnetic field lines from observed field line resonance frequencies. Using the T01 magnetic field model, we have shown that the extent to which field line eigenfrequencies depend on field line geometry is significant. By assuming a constant plasma mass density everywhere in the magnetosphere, effects on field line eigenfrequencies due to local time and the level of geomagnetic activity are apparent. A comparison of mass density computed assuming a dipole versus the density computed using T01 shows that the dipole assumption results in an overestimation of mass density. This overestimation is larger for larger densities, L shells, and *Dst*.

[26] Mass density determined from FLRs can be useful for inferring the presence of heavy ions in the magnetosphere when combined with measurements of electron number density [e.g., *Berube et al.*, 2005; *Fraser et al.*, 2005; *Takahashi et al.*, 2004; *Dent et al.*, 2003]. The ratio of mass density to electron density gives the average ion mass. An increase in average ion mass could imply an increase in the number of heavy ions. The overestimation of mass density due to the dipole assumption found by the current study implies an overestimation of heavy ion mass loading by studies that use the FLR technique in general. This overestimation is greater during disturbed times. Our results indicate that mass density determined from FLRs assuming a dipole magnetic field will result in the inference of a greater number of heavy ions than are actually present, especially during disturbed times. A more detailed investigation of plasma mass density and heavy ion dynamics during geomagnetic storms using the new time-dependent Tsyganenko magnetic field model [*Tsyganenko and Sitnov*, 2005] is the topic of a future study.

[27] It is important to consider the effects of field line geometry on FLRs, even in the inner magnetosphere ($L \sim 3$), where the dipole assumption is often considered to be valid even during storms. A realistic representation of the magnetospheric magnetic field is essential for accurately determining the mass density along magnetic field lines.

[28] **Acknowledgments.** This work was supported by NSF grant (ATM-0348398) and a NASA GSRP fellowship (NGT5-117).

[29] Lou-Chuang Lee thanks Kazue Takahashi and James Wanliss for their assistance in evaluating this paper.

References

Baransky, L. N., J. E. Borovkov, M. B. Gokhberg, S. M. Krylov, and V. A. Troitskaya (1985), High resolution method of direct measurement of the magnetic field lines' eigenfrequencies, *Planet. Space Sci.*, *33*(12), 1369.

Baransky, L. N., S. P. Belokris, Y. E. Borovkov, M. B. Gokhberg, N. Federov, and C. A. Green (1989), Restoration of the meridional structure of geomagnetic pulsation fields from gradient measurements, *Planet. Space Sci.*, *37*(7), 859.

Berube, D., M. B. Moldwin, and J. M. Weygand (2003), An automated method for the detection of field line resonance frequencies using ground magnetometer techniques, *J. Geophys. Res.*, *108*(A9), 1348, doi:10.1029/2002JA009737.

Berube, D., M. B. Moldwin, S. F. Fung, and J. L. Green (2005), A plasmaspheric mass density model and constraints on its heavy ion concentration, *J. Geophys. Res.*, *110*, A04212, doi:10.1029/2004JA010684.

Cummings, W. D., R. J. O'Sullivan, and P. J. Coleman (1969), Standing Alfvén waves in the magnetosphere, *J. Geophys. Res.*, *74*(3), 778.

Dent, Z. C., I. R. Mann, F. W. Menk, J. Goldstein, C. R. Wilford, M. A. Clilverd, and L. G. Ozeke (2003), A coordinated ground-based and IMAGE satellite study of quiet-time plasmasphere density profiles, *Geophys. Res. Lett.*, *30*(12), 1600, doi:10.1029/2003GL016946.

Denton, R. E., M. R. Lessard, R. Anderson, E. G. Miftakhova, and J. W. Hughes (2001), Determining the mass density along magnetic field lines from toroidal mode eigenfrequencies: Polynomial expansion applies to CRRES data, *J. Geophys. Res.*, *106*(A12), 20,915.

Fraser, B. J., J. L. Horwitz, J. A. Slavin, Z. C. Dent, and I. R. Mann (2005), Heavy ion mass loading of the geomagnetic field near the plasmapause and ULF wave implications, *Geophys. Res. Lett.*, *32*, L04102, doi:10.1029/2004GL021315.

Gallagher, D. L., P. D. Craven, and R. H. Comfort (2000), Global core plasma model, *J. Geophys. Res.*, *105*(A8), 18,819.

Goldstein, J., R. E. Denton, M. K. Hudson, E. G. Miftakhova, S. L. Young, J. D. Menietti, and D. L. Gallagher (2001), Latitudinal density dependence of magnetic field lines inferred from Polar plasma wave data, *J. Geophys. Res.*, *106*(A4), 6195.

Hattingh, S. K. F., and P. R. Sutcliffe (1987), Pc3 pulsation eigenperiod determination at low latitudes, *J. Geophys. Res.*, *92*(A11), 12,433.

Kawano, H., K. Yumoto, V. A. Pilipenko, Y.-M. Tanaka, S. Takasaki, M. Iizima, and M. Seto (2002), Using two ground stations to identify magnetospheric field line eigenfrequency as a continuous function of ground latitude, *J. Geophys. Res.*, *107*(A8), 1202, doi:10.1029/2001JA000274.

Menk, F. W., D. Orr, M. A. Clilverd, A. J. Smith, C. L. Waters, D. K. Milling, and B. J. Fraser (1999), Monitoring spatial and temporal variations in the dayside plasmasphere using geomagnetic field line resonances, *J. Geophys. Res.*, *104*(A9), 19,955.

Orr, D., and J. A. D. Matthew (1971), The variation of geomagnetic micropulsation periods with latitude and the plasmapause, *Planet. Space Sci.*, *19*, 897.

Pilipenko, V. A., and E. N. Federov (1994), Magnetotelluric sounding of the crust and hydrodynamic monitoring of the magnetosphere with the use of ULF waves, in *Solar Wind Sources of Magnetospheric Ultra-Low-Frequency Waves*, *Geophys. Monogr. Ser.*, vol. 81, edited by M. J. Engebretson, K. Takahashi, and M. Scholer, pp. 283–292, AGU, Washington, D. C.

Price, I. A., C. L. Waters, F. W. Menk, G. J. Bailey, and B. J. Fraser (1999), A technique to investigate plasma mass density in the topside ionosphere using ULF waves, *J. Geophys. Res.*, *104*, 12,723.

Rankin, R., and V. T. Tikhonchuk (2001), Dispersive shear Alfven waves on model Tsyganenko magnetic field lines, *Adv. Space Res.*, *28*(11), 1595.

Reinisch, B. W., X. Huang, P. Song, G. S. Sales, S. F. Fung, J. L. Green, D. L. Gallagher, and V. M. Vasilyuas (2001), Plasma density distribution along the magnetospheric field: RPI observations from IMAGE, *Geophys. Res. Lett.*, *28*(24), 4521.

Singer, H. J., D. J. Southwood, R. J. Walker, and M. G. Kivelson (1981), Alfven wave resonances in a realistic magnetospheric magnetic field geometry, *J. Geophys. Res.*, *86*(A6), 4589.

Takahashi, K., and R. L. McPherron (1982), Harmonic structure of Pc 3-4 pulsations, *J. Geophys. Res.*, *87*(A3), 1504.

Takahashi, K., R. E. Denton, R. R. Anderson, and W. J. Hughes (2004), Frequencies of standing Alfven wave harmonics and their implication for plasma mass distribution along magnetic field lines: Statistical analysis of CRRES data, *J. Geophys. Res.*, *109*, A08202, doi:10.1029/2003JA010345.

Troitskaya, V. A., and A. V. Gul'elmi (1967), Geomagnetic micropulsations and diagnostics of the magnetosphere, *Space Sci. Rev.*, *7*, 689.

Tsyganenko, N. A. (2002a), A model of the near magnetosphere with a dawn-dusk asymmetry 1. Mathematical structure, *J. Geophys. Res.*, *107*(A8), 1179, doi:10.1029/2001JA000219.

Tsyganenko, N. A. (2002b), A model of the near magnetosphere with a dawn-dusk asymmetry 2. Parameterization and fitting to observations, *J. Geophys. Res.*, *107*(A8), 1176, doi:10.1029/2001JA000220.

Tsyganenko, N. A., and M. I. Sitnov (2005), Modeling the dynamics of the inner magnetosphere during strong geomagnetic storms, *J. Geophys. Res.*, *110*, A03208, doi:10.1029/2004JA010798.

Tsyganenko, N. A., H. J. Singer, and J. C. Kasper (2003), Storm-time distortion of the inner magnetosphere: How severe can it get?, *J. Geophys. Res.*, *108*(A5), 1209, doi:10.1029/2002JA009808.

Wanliss, J. A., R. Rankin, J. C. Samson, and V. T. Tikhonchuk (2002), Field line resonances in a stretched magnetotail: CANOPUS optical and magnetometer observations, *J. Geophys. Res.*, *107*(A7), 1100, doi:10.1029/2001JA000257.

Waters, C. L., F. W. Menk, B. J. Fraser, and P. M. Oswald (1991), Phase structure of low-latitude Pc 3-4 pulsations, *Planet. Space Sci.*, *39*(4), 569.

Waters, C. L., J. C. Samson, and E. F. Donovan (1995), The temporal variation of the frequency of high latitude field line resonances, *J. Geophys. Res.*, *100*(A5), 7987.

Waters, C. L., J. C. Samson, and E. F. Donovan (1996), Variation of plasmatrough density derived from magnetospheric field line resonances, *J. Geophys. Res.*, *101*(A11), 24,737.

M. Ahn, D. Berube, and M. B. Moldwin, Department of Earth and Space Sciences, University of California, Los Angeles, 3845 Slichter Hall, P. O. Box 951567, Los Angeles, CA 90095-1567, USA. (dberube@igpp.ucla.edu)